Volume scattering function of suspended particulate matter at near-forward angles: a comparison of experimental and theoretical values

Richard W. Spinrad, J. Ronald V. Zaneveld, and Hasong Pak

Narrow angle light scattering measurements were made for various sizes of spherical particles suspended in water. These were compared to calculated theoretical scattering values as derived from the theory of Mie (1908). Through measurements with different particle concentrations at angles between 0.2° and 0.7° the effect of the unscattered main beam light was removed. Results agreed well with Mie theory for these angles.

Introduction

The measurement of the volume scattering function $\beta(\theta)$ of suspended particulate matter in water at very small angles is a problem which has received considerable attention in the past.[1-19] The importance of this measurement lies in the fact that more than half of all scattered radiant intensity is scattered at angles less than 3° from the incident main beam.[20] The measurement of volume scattering functions at near-forward angles may also be used in conjunction with particle size analysis and scattering measurements at midrange angles for the determination of the index of refraction of nonabsorbing particles.[21,22] In addition, visibility in the sea will be affected by forward scattering as shown by Wells *et al.*[3]

A theoretical representation of scattering of electromagnetic waves by spherical, nonabsorbing particles was presented by Mie.[23] This theory, which is employed for this experiment, indicates that the volume scattering function $\beta(\theta)$, for a system of spherical particles, all having the same diameter and index of refraction, is relatively constant over a range of small angles (Fig. 1 from the values in Salganik and Shifrin[24]). The angle θ at which $\beta(\theta)$ begins to decrease noticeably varies with particle size, being larger for the smaller particles. Also, at angles less than approximately 1°, a larger particle will scatter a greater amount of radiant intensity than a smaller one. The theoretical values used in this experiment were obtained from the tables of Salganik and Shifrin.[24] These tables were used because they provided the most values for theoretical scattering at angles less than 1° for a variety of particle sizes. Other references[18,19] do not contain as extensive a listing of narrow angle scattering functions.

Previous workers have obtained scattering curves which differed significantly from the theoretical values for small angles ($0° < \theta < 1°$). Morrison[1] used a small angle scattering meter which took readings at approximately 0.2°, 0.6°, and 1.2°. The curves obtained of $\beta(\theta)$ vs θ show a decrease of more than 2 orders of magnitude in $\beta(\theta)$ from $\theta = 0.1°$ to $\theta = 1°$. [$\beta(\theta)$ for $\theta <$ 0.2° was interpolated in his curves.] Wells *et al.*[3] measured a point spread function and got results very similar to those of Morrison. Hodara[2] described measurements of $\beta(\theta)$ via modulation transfer function (MTF) measurements. The results he obtained with an MTF meter agreed well with theoretical results only at angles greater than 2°. At small angles the values obtained were much larger than theory predicts. In these experiments possible lack of collimation, inclusion of main beam radiant intensity, and insufficient data points at angles less than 1° could be the causes for the discrepancies between theory and experiment. Honey and Sorenson[13] concluded that turbulent fluctuations in the refractive index of water would contribute significantly to scattering only at angles less than 200 μrad. The experiment described herein was performed in a much larger angular region, so turbulence induced scattering may be ignored. In this experiment, results have been obtained that agree very well with the Mie theory values obtained by Salganik and Shifrin[24] over the small angle region. Values of $\beta(\theta)$ and slopes of $\beta(\theta)$ vs θ obtained experimentally correspond very closely to

The authors are with Oregon State University, School of Oceanography, Corvallis, Oregon 97331.

Received 5 March 1977.
0003-6935/78/0401-1125$0.50/0.

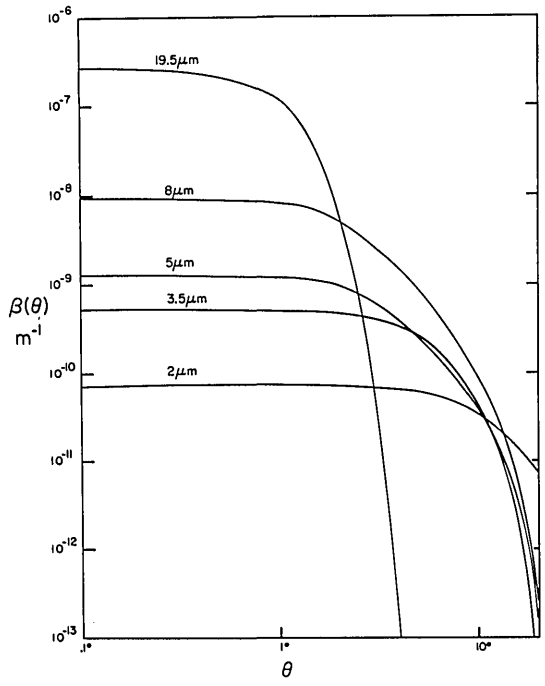

Fig. 1. Theoretical scattering values $\beta(\theta)$ for 1 particle/m^3 and for diameters indicated. Values were obtained from Salganik and Shifrin.[24] θ is the angle from the main beam. Particles have an index of refraction of 1.15 relative to pure water.

theoretical calculations. The reason this experiment can substantiate theory effectively is that the effects of the main beam (i.e., unscattered radiant intensity) can be removed through multiple measurements, as explained in the theoretical portion of this paper. Also, the experimental setup was such that the collimation angle of the receiver was reduced to approximately 1 μsr by using a small receiver area.

Theory

The appearance of unscattered light from the finite main beam must be considered in any small angle optical measurement. In addition, it must be realistically assumed that the direct light is not perfectly collimated and that there may be some scattering from the lenses in the optical setup. Therefore, as shown in Fig. 2, the power received P_r will be equal to the power received due to scattering P_β plus the noise P_n due to main beam inclusion, lack of collimation, and scattering from the lenses;

$$P_r = P_\beta + P_n. \tag{1}$$

The volume scattering function is defined as

$$\beta(\theta) = [dI(\theta)]/(E dv) \quad \text{(Jerlov[20])}, \tag{2}$$

where $dI(\theta)$ = scattered radiant intensity at angle θ (w/sr),
E = incident irradiance (w/m^2), and
dv = volume element from which $dI(\theta)$ is scattered (m^3).

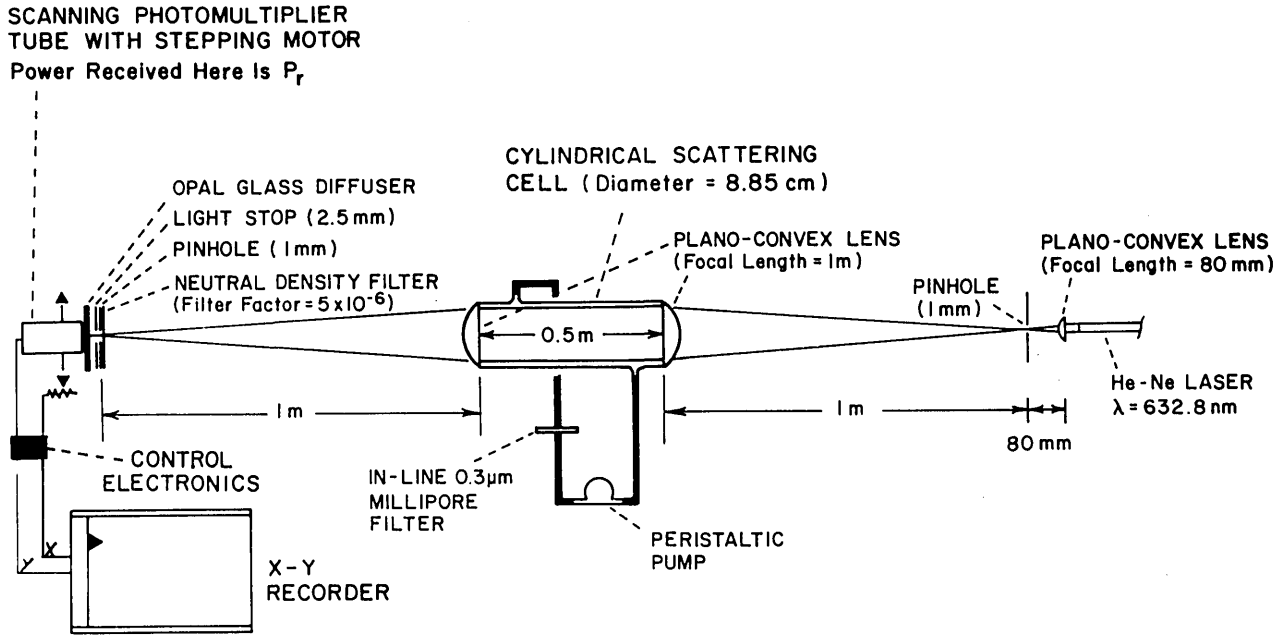

Fig. 2. Schematic drawing of the laboratory setup of the small angle scattering meter.

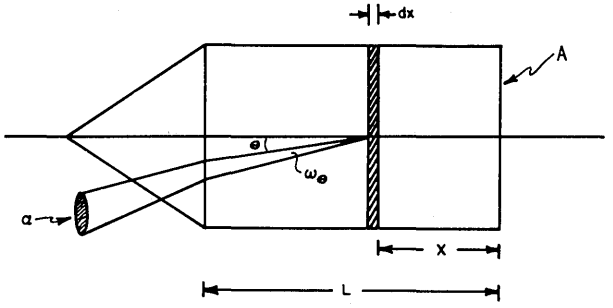

Fig. 3. An elementary scattering volume Adx scattering light with the solid angle w_θ at an angle θ from the main beam.

Consider Fig. 3, which shows an elementary scattering volume spaced on the center line of the apparatus,

$$dI(\theta) = \{dP_\beta \exp[c(L - x)]/w_\theta, \tag{3}$$

where dP_β = power received due to scattering from the volume element dv, c = total attenuation coefficient, and w_θ = the solid angle subtended by the receiver:

$$E = [P_0 \exp(-cx)]/A. \tag{4}$$

Therefore,

$$\beta(\theta) = \frac{dP_\beta \exp[c(L - x)]}{w_\theta \dfrac{P_0 \exp(-cx)}{A} Adx} \tag{5}$$

and

$$dP_\beta = \beta(\theta) w_\theta P_0 \exp(-cL). \tag{6}$$

Integration of dP_β over the length of the cell yields total scattered power received due to particulate matter and water:

$$P_\beta = \int_0^L dP_\beta dx = \beta(\theta) w_\theta P_0 L \exp(-cL). \tag{7}$$

Total received power can therefore be expressed as

$$P_r = P_n + \beta(\theta) w_\theta P_0 L \exp(-cL). \tag{8}$$

Furthermore, the scattering function $\beta(\theta)$ can be divided into scattering due to water $\beta_w(\theta)$:

$$\beta(\theta) = \beta_p(\theta) + \beta_w(\theta), \tag{9}$$

$$P_r = P_n + [\beta_p(\theta) + \beta_w(\theta)] w_\theta P_0 L \exp(-cL). \tag{10}$$

By increasing particle concentration by a factor F, the particle scattering function will also increase by a factor F. That is, scattering is additive provided multiple scattering does not occur.[25] (The cell volume and the particle concentrations were such that multiple scattering was insignificant in this experiment.) For the first concentration of particles

$$P_{r1} = P_{n1} + [\beta_p(\theta) + \beta_w(\theta)] w_\theta P_0 L \exp(-c_1 L), \tag{11}$$

and for the second concentration of particles

$$P_{r2} = P_{n1} \exp[-(c_2 - c_1)L] + [F\beta_p(\theta) + \beta_w(\theta)] w_\theta P_0 L \exp(-c_2 L). \tag{12}$$

The noise P_{n1} received during the first measurement will be reduced with the addition of particles. This reduction is equal to the ratios of the transmissivities of the two concentrations. The transmissivities are defined as

$$T_1 = \exp(-c_1 L),$$

$$T_2 = \exp(-c_2 L),$$

$$P_{n2} = P_{n1} \frac{\exp(-c_2 L)}{\exp(-c_1 L)} = P_{n1} \exp[-(c_2 - c_1)L]. \tag{13}$$

Multiplying Eq. (11) by $\exp[-(c_2 - c_1)L]$ and subtracting Eq. (12) yield

$$P_{r1} \exp[-(c_2 - c_1)L] - P_{r2} = [\beta_p(\theta) + \beta_w(\theta)] w_\theta P_0 L \exp(-c_2 L) - [F\beta_p(\theta) + \beta_w(\theta)] w_\theta P_0 L \exp(-c_2 L) \tag{14}$$

$$= (1 - F)\beta_p(\theta) w_\theta P_0 L \exp(-c_2 L), \tag{15}$$

$$\beta_p(\theta) = \frac{P_{r1}(\theta) \exp(c_1 L) - Pr_2(\theta) \exp(c_2 L)}{(1 - F) w_\theta P_0 L}. \tag{16}$$

Using the transmissivities as defined by

$$T_1 = \exp(-c_1 L) = [P_{r1}(°)]/P_0, \tag{17}$$

$$T_2 = \exp(-c_2 L) = [P_{r2}(0)]/P_0. \tag{18}$$

Equation (16) can be simplified as

$$\frac{\dfrac{P_{r_1}(\theta)}{P_{r_1}(0)} - \dfrac{P_{r_2}(\theta)}{P_{r_2}(0)}}{(1 - F) w_\theta L}. \tag{19}$$

Thus, with two measurements at different particle concentrations, the particle scattering function can be calculated.

Experimental Setup

A schematic representation of the narrow angle scattering meter is shown in Fig. 2. The water in the cell was kept nearly particle-free by filtration through an in-line 0.3-μm millipore filter. In front of the He–Ne laser was a planoconvex lens which focused the laser light onto a pinhole 80 mm away. This lens–pinhole combination provided a point source of light to facilitate collimation of the beam within the scattering cell. The planoconvex lens on the right side of the cell was placed exactly one focal length from the pinhole. On the left side of the cell another planoconvex lens focused the beam down onto another pinhole through a neutral density filter. A light stop was placed behind the pinhole to align the beam onto the photomultiplier tube, and an opal glass diffuser was placed behind the stop in order to utilize a larger area of the photomultiplier tube. The signal received by the PM tube was used to drive the Y axis of the X -Y recorder. The X axis indicated displacement of the platform on which the photomultiplier tube was mounted. The tube was first placed in the path of the main beam to obtain the value of $P_r(0)$. With a motor driving the platform, the tube then scanned the region from 0.2° to 0.7° relative to the center of the main beam to obtain the values of $P_r(\theta)$ for $0.2° \leq \theta \leq 0.7°$. A reference angle was obtained on the X -Y recorder by scanning the main beam with the

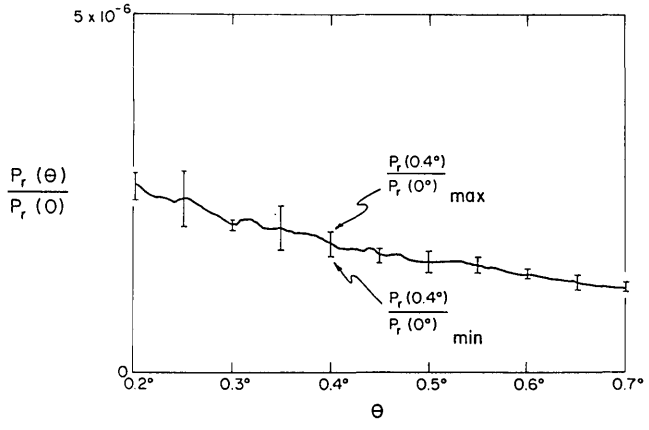

Fig. 4. Experimental results obtained with the narrow angle scattering meter showing the maximum and minimum values of $[P_r(\theta)]/[P_r(0)]$ for eleven values of θ and the mean value over the complete angular range. $P_r(\theta)$ is the power received at an angle θ from the main beam. $P_r(0)$ is the power received at 0° from the main beam.

photomultiplier tube. The resultant peak on the recorder had a plane angular width equal to that of the pinhole in front of the photomultiplier tube. The pinhole with a 1-mm diam was placed 1 m from the lens. The plane angle it subtended was therefore 0.033°. The X-Y recorder was thus calibrated for angular determinations. The solid angle subtended by the pinhole [w_θ in Eq. (19)] was 0.79×10^{-6} sr.

Particles were introduced into the cell with a syringe, and the water was stirred to produce a homogeneous scattering medium. After each scattering measurement the water was filtered until the standard clean water scattering level was attained to assure cleanliness of the water in the cell. This scattering level amounted to less than 5% of the level obtained for the samples containing particles.

A 300-ml stock solution of suspended particles was prepared for each of the three particle sizes (mean diameters of 5.2 μm, 8 μm, and 9.8 μm). The spherical particles were a copolymer of styrene and divinyl benzene. The particles have an index of refraction of 1.15 relative to water and the standard deviations from the mean diameters are as follows: 7% for the 5.2-μm particles; 15% for the 8-μm particles; and 12.5% for the 9.8-μm particles. Forty drops of the particle supplies were added to 300 ml of filtered (through a 0.3-μm filter) distilled water to make the stock solution. A size distribution analysis was performed using a resistance pulse counter (composed of Coulter glassware and a Nuclear Data pulse height analyzer) five times for each of the three stock solutions. Ten milliliters of stock solution were added to the clean, filtered water in the cell in the narrow angle meter, and five continuous scattering profiles from 0.2° to 0.7° were taken successively. The water was again filtered until clean (as defined by the clean water standard), and then 20 ml of stock solution were added to the cell, and five more successive profiles were taken. This whole process was performed for each of the three particle sizes. The size distributions obtained were used to calculate the theoretical volume scattering functions for each sample. The size distribution was broken up into channels in the pulse height analyzer or diameter ranges, the means of which corresponded to the diameters for which Salganik and Shifrin[24] calculated the theoretical scattering values needed to complete the total theoretical volume scattering function. The scattering value for a single particle of a given size was multiplied by the number of particles in the diameter range having a mean diameter of that same size. This was done for every diameter range to obtain the total theoretical volume scattering function. By limiting the size of the channels the error caused by using the mean diameter of a channel was only 2–3%.

Results

Each set of five experimental runs on the narrow angle scattering meter gave a maximum, a minimum, and three intermediate values of $P_r(\theta)/P_r(0)$ (Fig. 4) for any given value of θ. (The maximum and minimum are shown for each of eleven values of θ along with a continuous mean value for θ from 0.2° to 0.7°.) These values defined the experimental maxima and minima of the volume scattering functions. In addition, the particle counter indicated a maximum and a minimum number of particles for any given size range. This defined the theoretical maxima and minima of the volume scattering functions. The graphs of the experimental and theoretical volume scattering functions obtained (maxima and minima) vs θ for the three different size distributions used are shown in Figs. 5, 6, and 7. Noise levels are less than 5% in all three cases. The curves demonstrate a significant overlap between theoretical and experimental values of $\beta(\theta)$ for all values of θ measured. The slopes of theoretical and experimental values are very nearly parallel in all cases.

Discussion and Conclusion

The narrow angle scattering meter can effectively measure the scattered radiant intensity at angles less than 0.7°. The results obtained indicate that the behavior of scattered light as predicted by Mie[23] is in fact a verifiable phenomenon. The flatness of the curve of $\beta(\theta)$ vs θ is seen experimentally and theoretically. The averaged results of this experiment are qualitatively compared to those of other experimentalists and to theory (normalized at 0.5°) in Fig. 8. The experimental and theoretical values do coincide to a great extent. These values were taken from five test runs for each particle size distribution. Statistically, it would be best to take a much greater number of test runs for each particle size distribution. This would probably bring the experimental and theoretical curves into closer agreement. This was made evident after the initial experiment when only one test run was made for each concentration of a given particle size. Results were scattered above and below what theory predicted. By

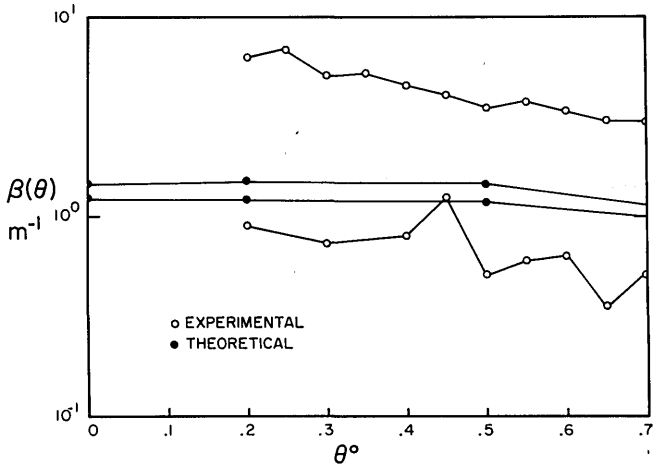

Fig. 5. Theoretical and experimental scattering maxima and minima at small angles for suspended particles of 5.2-μm diam.

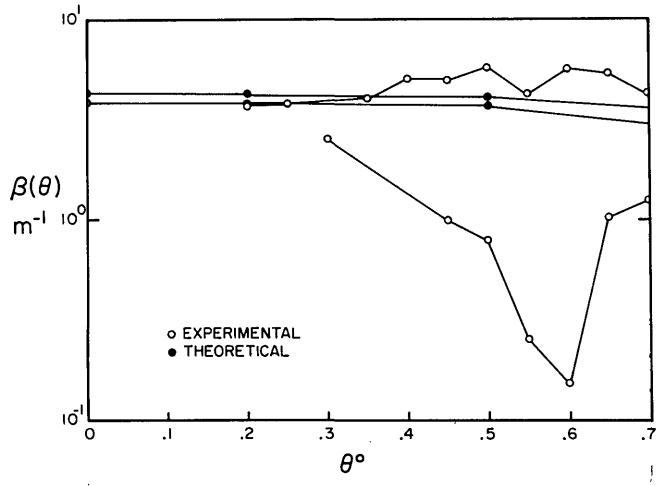

Fig. 6. Theoretical and experimental scattering maxima and minima at small angles for suspended particles of 8-μm diam.

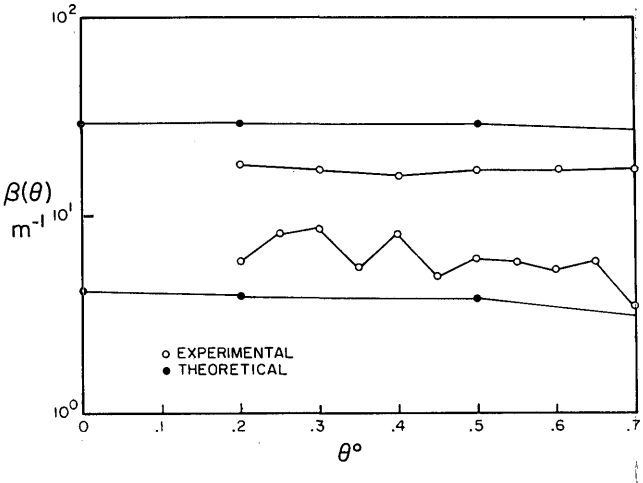

Fig. 7. Theoretical and experimental scattering maxima and minima at small angles for suspended particles of 9.8-μm diam.

using five test runs the average became much closer to the theoretical values. This suggests that by further increasing the number of test runs, the experimental results should come even closer to theoretical predictions. Discrepancies and anomalies in the curves may be explained by a variety of reasons: inhomogeneous particle concentrations in the particle counter sample or in the narrow angle scattering meter cell; additional particles in the cell which were not in the water used for particle counter work (e.g., dust or microbubbles); human error in the measurement of particle stock solution added to the cell.

A scattering profile [$\beta(\theta)$ vs θ for $0° < \theta < 180°$] for a sample of water containing suspended particulate matter will vary depending on the particle size distribution, the particles' shapes, and the index of refraction of the particles. By use of scattering meters at near forward angles, midrange angles, and angles greater than 90°, together with a particle size analyzer such as a Coulter counter, it may be possible to determine the relative composite index of refraction of a given sample of suspended particles.[21,22,26]

The authors thank Robert Bartz for his work in the design, development, and fabrication of the narrow angle scattering meter and Carol Stiefvater for typing the manuscript. Support from the Office of Naval Research through contract N00014-76-C-0067 under project NR 083-102 is gratefully acknowledged. We also thank T. J. Petzold for his helpful suggestions for the development of the narrow angle scattering meter.

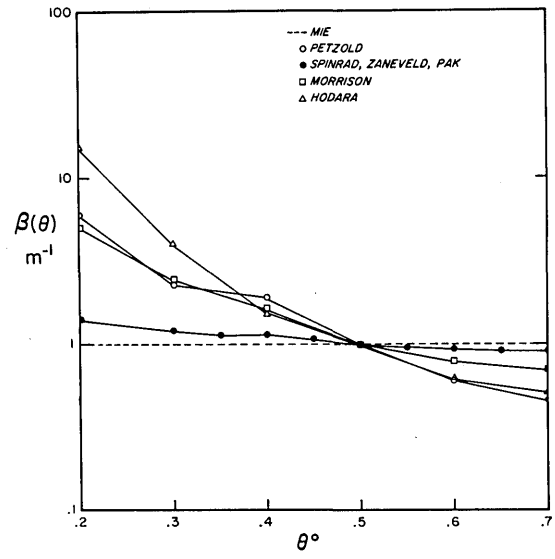

Fig. 8. A qualitative comparison of mean scattering results obtained in this experiment, results of previous experiments, and the theoretical results obtained from the theory of Mie,[23] normalized to $\beta(\theta) = 1\ m^{-1}$ at $\theta = 0.5°$.

References

1. R. E. Morrison, "Studies on the Optical Properties of Seawater, Argus Island in the North Atlantic Ocean and in Long Island and Block Island Sounds," Ph.D. Thesis, New York U., New York (1967).
2. H. Hodara, AGARD Lecture Series 61 on Optics of the Sea, Neuilly Sur Seine, France (1973).
3. W. Wells, H. Hodara, and O. Wilson, "Long Range Vision in Sea Water," Final Report ARPA order 1737, Tetra Tech. Inc., Pasadena, Calif. (1972).
4. L. Mertens, and W. Wells, As described by H. Hodara, Ed., AGARD Lecture Series 61 on Optics of the Sea, Neuilly Sur Seine, France (1973).
5. S. Q. Duntley, J. Opt. Soc. Am. **53**, 214 (1963).
6. G. Kullenberg, Deep Sea Res. **15**, 423 (1968).
7. D. Bauer and A. Morel, Ann. Geophys. **23**, 109 (1967).
8. R. N. Sokolov, F. A. Kudravitskii, and G. D. Petrov, Izv. Atmos. Oceanic Phys. **7**, 1015 (1971).
9. T. J. Petzold, SIO Ref. 72-78, 79 pp. (1972).
10. W. R. McCluney, Appl. Opt. **13**, 548 (1974).
11. D. Bauer and A. Ivanoff, Compte Rend. Acad. Sci. Paris **260**, 631 (1965).
12. E. J. Softley and J. F. Dilley, in *Ocean 72. IEEE International Conference of Engineering in the Ocean Environment,* Newport (1972).
13. R. C. Honey and G. P. Sorenson, AGARD Conf. Proc. No. 77, 39-39.7 (1970).
14. A. Morel, J. Chem. Phys. **10**, 1359 (1966).
15. M. V. Kozlyaninov, Tr. Inst. Okeanol., Akad. Nauk SSR **25**, 134 (1957).
16. Y. E. Ochakovsky, U.S. Dept. Comm., Joint Publ. Res. Ser., Rep. 36(816), 98-105 (1966).
17. F. Nyfeller, AGARD Conf. Proc. No. 77, 31-1-8 (1970).
18. A. Morel, Rapport 10, CNRS (1973).
19. O. B. Brown and H. R. Gordon, U. Miami, Pub. MIAPHOP-71.5 (1971).
20. N. G. Jerlov, *Marine Optics* (Elsevier, New York, 1970), 231 pp.
21. J. R. V. Zaneveld and H. Pak, J. Opt. Soc. Am. **63**, 321 (1973).
22. J. R. V. Zaneveld, D. M. Roach, and H. Pak, J. Geophys. Res. **79**, 4536 (1974).
23. G. Mie, Ann. Phys. **25**, 377 (1908).
24. I. N. Salganik and K. S. Shifrin, *Light Scattering Tables* (USSR Academy of Sciences, P. P. Shirskov Institute of Oceanography Leningrad, 1973).
25. H. C. Van De Hulst, *Light Scattering by Small Particles* (Wiley, New York, 1957, 470 pp.
26. H. R. Gordon and O. B. Brown, Trans. Am. Geophys. Union **52**, 245 (1971).

short summer courses for scientists

and engineers

Institute of Optics, University of Rochester, Rochester, New York 14627. Contact Nicholas George 716-275-2314

OPTICAL SYSTEM DESIGN June 19 - 23

Rudolf Kingslake's course is designed to give participants sufficient acquaintance with the various types of optical elements so that they can lay out a system to fit into the space available and perform the specified task. Lens design is not covered. Lectures are Monday through Thursday. On Friday morning there will be an optional visit to a local optical firm, Tropel, Inc., for demonstrations of sophisticated optical testing equipment such as an OTF measuring system and digital surface testing interferometer, and a tour of a modern production optical shop. Tuition fee is $395.